Mol. Cryst. Liq. Cryst., Vol. 544: pp. 37/[1025]–49/[1037], 2011

ISSN: 1542-1406 print/1563-5287 online
DOI: 10.1080/15421406.2011.569265

Taylor & Francis
Taylor & Francis Group

Uniform Lying Helix Alignment on Periodic Surface Relief Structure Generated via Laser Scanning Lithography

GIOVANNI CARBONE, DANIEL CORBETT, STEVE J. ELSTON, PETER RAYNES, ALEXANDER JESACHER, RICHARD SIMMONDS, AND MARTIN BOOTH

Department of Engineering Science, University of Oxford, United Kingdom

The main drawback in the exploitation of the chiral-flexo-electro-optic effect is that it relies on a texture, the Uniform Lying Helix (ULH), which is unstable when the cholesteric is sandwiched between spatially uniform aligning surfaces (UASs). It has been shown that the ULH can be promoted by periodic (horizontal/vertical) anchoring conditions or by the presence of periodic polymeric walls. Here we show that periodic surface relief structures can also promote the formation of a stable ULH texture. The surface relief structure was created by curing an ultraviolet curable material via a two-photon excitation laser-lithography process. The process allows sub-micron resolution and flexibility in creating the topographic relief.

Keywords Electro-optic; flexoelectricity; liquid crystals application; polymer structure; surface structure

1. Introduction

Flexoelectricity in a nematic liquid crystal, first predicted by Meyer [1] in 1969, is the coupling between the elastic distortion of the director and the electric polarization. It can be shown using symmetry arguments that only bend and splay distortion produce a non-zero electric polarization $\vec{P}$, which can be expressed as

$$\vec{P} = e_1\hat{n}(\nabla \cdot \hat{n}) - e_3\hat{n} \times (\nabla \times \hat{n}) \tag{1}$$

where $\hat{n}$ is the nematic director and the coupling coefficients e_1 and e_3 are respectively the splay and bend flexoelectric coefficients.

An interesting consequence of the flexoelectric coupling is the so called chiral flexo-electro-optic (FEO) effect [2], which is observed in a short pitch cholesteric aligned in the uniform lying helix (ULH) texture. The ULH refers to a uniformly aligned parallel-plate cell in which the helical axis of a cholesteric lies parallel to

Address correspondence to Giovanni Carbone, (current address) Micron Technology, Inc., 2602 Clover Basin Dr., Longmont, CO 80304, USA. Tel.: +1-303-7742218; E-mail: gcarbone@micron.com

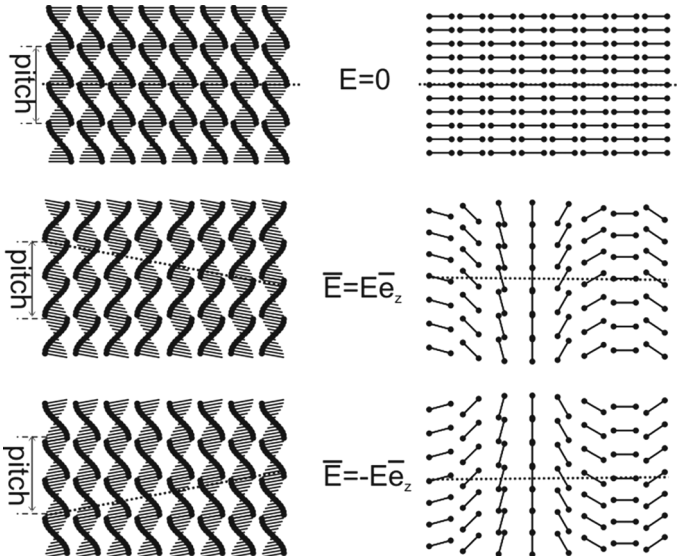

Figure 1. In the presence of an electric field, the projection of the director on a plane perpendicular to the optical axis describes a periodic bend-splay pattern which produces a flexoelectric polarization that couples with the electric field.

the confining surfaces in a unique direction. A short pitch cholesteric is optically uniaxial, with the optical axis parallel to the cholesteric helix such that an aligned ULH slab acts like a retardation plate.

In the FEO effect an electric field E, applied perpendicular to the helix induces an in-plane tilt of the optical axis of a short-pitch cholesteric aligned in the ULH (see Fig. 1). The magnitude of the tilt is proportional to the electric field, and the tilt is inverted if the polarity of the electric field is reversed.The flexo-electric nature of the tilt becomes apparent if one considers the projection of the nematic director on a plane Γ perpendicular to the optical axis. As shown in Figure 1, in the absence of an electric field the tilt is zero and the director projection on Γ is homogeneous, but for a tilt different from zero, one can easily identify a periodic splay bend distortion of the nematic director in Γ. The flexo-electric polarization arising from such distortion couples with the electric field causing the tilt. If the tilt φ is assumed constant throughout the cell, it can be shown that

$$\tan\phi = \frac{ep}{2\pi k}E \tag{2}$$

where p is the cholesteric pitch, k is an average elastic constant, $e=(e_1-e_3)/2$ is the effective flexoelectric coefficient and E is the magnitude of the electric field.

The simple behaviour described in Eq. 2 is in general perturbed by the dielectric coupling which tends to unwind the cholesteric helix, limiting the linear regime of the FEO effect [3], however, an appropriate design of the liquid crystal (LC) molecules can substantially increase the range of linearity [4,5]. In the past 10 years, considerable improvement has been made in this direction and new LC mixtures, specifically designed for the FEO effect, have been synthesized, based on the use of bimesogenic

molecules [6–8]. These mixtures exhibit a large flexoelectric ratio e/k, and a relatively small dielectric constant $\Delta\varepsilon$ extending the linear range of the flexoelectric effect to angles as large as 30° [9]. Thus full modulation between dark and bright states is possible within the linear regime.

Linear effects in LCs are quite rare and potentially very interesting, since they allow fast changes in the optical state [10]. The case of the FEO effect is particularly interesting for many reasons. First of all, the response times are in the microsecond range for short pitch materials (it has to be noted that the use of pitch of around 300 nm is also necessary to avoid diffractive effects). In addition, the FEO can show great temperature independence, since both the average flexoelectric coefficients e and the average elastic constant k are believed to scale quadratically with the nematic order parameter S [3]. By choosing chiral LC mixtures with temperature compensated pitch, it is possible to obtain an electro-optic characteristic that is temperature independent [3,11]. This makes the FEO effect potentially useful for applications like wide viewing angle displays with grey-scale possibility, or sub-millisecond light shutters.

2. Uniform Lying Helix

In order to exploit the FEO effect in the display industry a few problems still need to be addressed, the most severe one is related to the ULH texture required. The ULH is intrinsically unstable since it is incompatible with both planar and homeotropic alignments. As a consequence, in order to accommodate the ULH close to a uniformly aligning surface a set of defect lines or a large periodic distortion need to be introduced close to the surface [12]. For positive dielectric anisotropy materials, one can force the ULH texture into the system by cooling down the sample from the isotropic phase, while applying a moderate electric field, but the texture is not ideal and, when rotated under crossed polarizers, the contrast ratio between dark and bright states is, in general, quite poor (see Fig. 2). Moreover, when the electric field is turned off, the system naturally relaxes back to the lower energy Grandjean texture, where the cholesteric helix is perpendicular to the confining surfaces. So far,

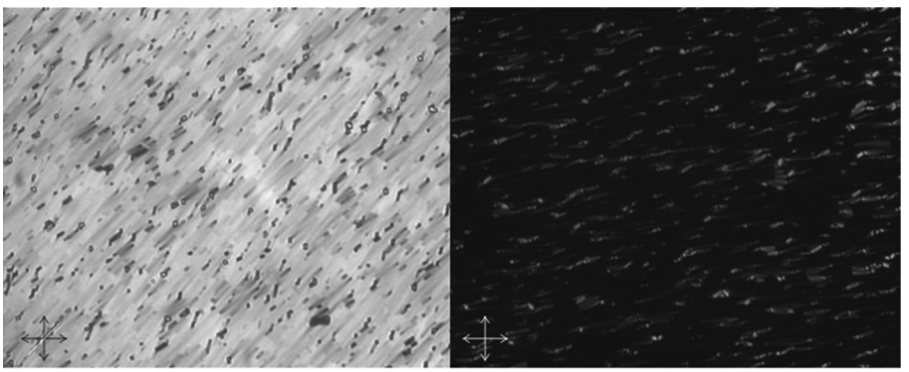

Figure 2. ULH alignment created by cooling a chiral nematic from the isotropic phase, while applying a moderate electric field. The optical axis is oriented (a) 45° and (b) 0° with respect to the polarizer.

only a few methods have been proposed to overcome this problem but a viable solution has still to be found.

In order to stabilize the ULH texture, the use of reactive mesogens has been proposed to create a polymeric structure that locks the cholesteric into the ULH texture [13–15]. The use of an appropriate concentration of reactive mesogens leads to stability of the ULH without having deterioration in the tilt magnitude or the switching speed. Nevertheless, this method relies on the good quality of a pre-existing ULH texture. This is usually achieved by mechanical shearing of the substrates, in order to induce a flow, while applying a moderate electric field through the cell, to uniformly align the helix axis in the plane of the device. This strategy can only be applied to align chiral nematics with positive dielectric anisotropy. Moreover, it is not viable to align devices in this way for industrial applications.

The use of a surface showing periodic (horizontal/vertical) anchoring conditions, initially proposed by Meyer [16], has also been used to produce ULH alignment [17]. Even though the idea is very interesting and allows the creation of a ULH without complex procedures such as mechanical shearing, the ULH texture does not naturally form on cooling from the isotropic phase and the application. An electric field needs to be used to favour the ULH creation.

It has been shown that the formation of a stable ULH can be promoted using periodic polymer walls [18]. In this paper we propose an alternative method, based on the use of periodic surface relief structure (SRS), to promote the formation of a stable ULH texture. The SRS are created via two photon laser scanning lithography [19].

3. Understanding the ULH Interface

In order to implement display applications which are based on the FEO effect, a robust method to produce a stable, uniform and reliable ULH texture needs to be developed. This can be better achieved by gaining a deeper understanding of the fundamental mechanisms taking place at the interface between the aligning surfaces and the bulk ULH. In previous work [12] we have studied the unwinding of the ULH texture in contact with a UAS and determined the director structure at the interface. To go further, here we consider the bulk ULH texture in contact with a UAS promoting a pretilt θ_0. Finite difference numerical simulation is used to evaluate the elastic free energy associated with the interface as the pretilt angle, θ_s is varied from $\theta_0 = 0$ (planar alignment) to $\theta_0 = \pi/2$ (homeotropic alignment). The resulting energy is compared with the elastic energy that the system would have if the ULH were replaced by a Grandjean texture. In the latter case, the free energy F is also evaluated by the approximate analytic solution $F = kq_0(1 - \cos\theta_s)$, where k is the average elastic constant and $q_0 = 2\pi/p$.

As shown in Figure 3, for all values of the pretilt, the Grandjean texture has a lower energy than the ULH texture, but the gap between the energies associated with the two textures has a maximum corresponding to the planar alignment and decreases with increasing pretilt. The energies in Figure 3 are evaluated in the absence of an electric field. If one considers a positive dielectric anisotropy material, an electric field applied perpendicular to the interface modifies the situation dramatically: in both cases it would increase the free energy, but, because the director corresponding to the Grandjean texture would always be perpendicular to the electric field, its free energy would increase more than in the case of the ULH.

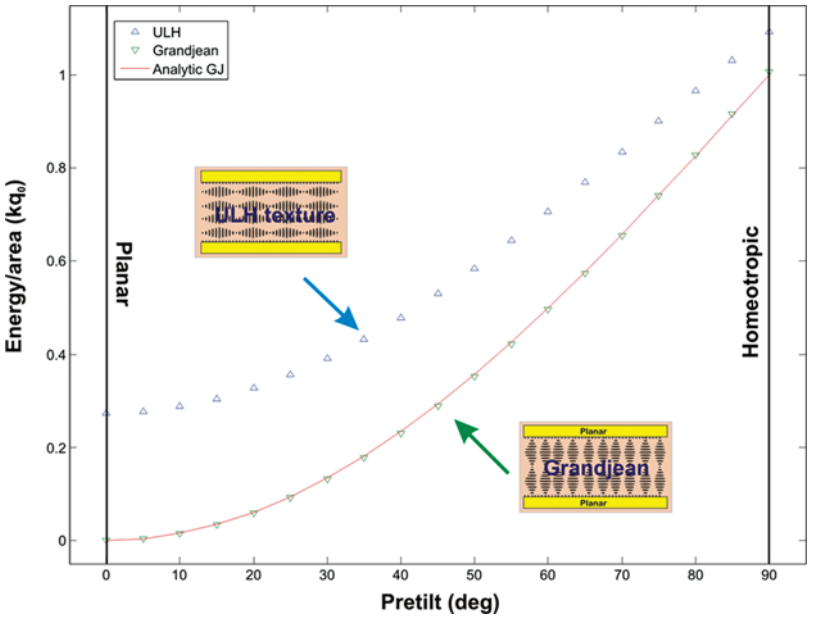

Figure 3. Elastic free energy of the interface region between a UAS and a bulk ULH (△) and between a UAS and a Grandjean (▽) as a function of the pretilt θ evaluated by finite difference numerical simulation. The continuous line is the analytic solution corresponding to the interface for the Grandjean texture. (Figure appears in color online.)

As a result, a ULH texture can be formed by applying an appropriate electric field. Unfortunately, even when it is formed, the ULH relaxes back to the Grandjean as the electric field is removed. An interesting fact, observed experimentally, is that large pretilt promotes metastability for ULH. Figure 4 shows the ULH texture, as observed in a microscope with crossed polarisers microscope, for a thin cholesteric film sandwiched between SiOx covered surfaces, inducing a 30 degree pretilt, and a rubbed polyimide, inducing a 60 degree pretilt. In both cases the texture is preserved for many days, even when the field is removed, but the ULH is lost if the temperature cycles through the isotropic phase or after the application of a large electric field which unwinds the helix.

The energies in Figure 3 are computed assuming rigid anchoring conditions. If weak anchoring is allowed, a correction to the free energy is necessary. In the case of weak homeotropic alignment, if the extrapolation of the anchoring is larger than the cholesteric pitch, it can be shown [20] that ULH has a lower energy than the Grandjean texture. Unfortunately, homeotropic alignment is not suitable to form the ULH since, due to its rotational symmetry, it does not define a direction for the helix.

4. Periodic Surface Relief Structure for ULH Alignment

As explained in the previous paragraph, both numerical simulation and textural observation of thin cholesteric films sandwiched between aligning substrates, suggest that weak homeotropic alignment promotes the formation of ULH. Because of the

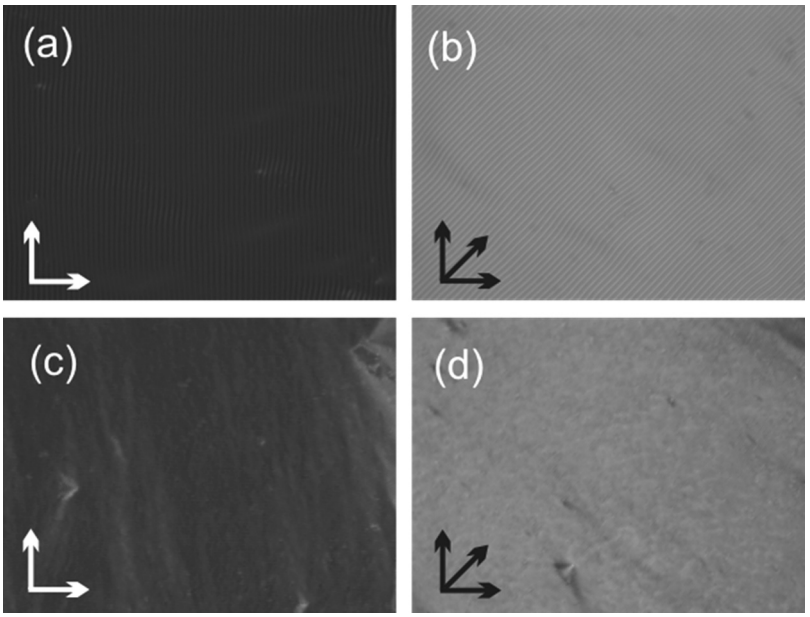

Figure 4. ULH texture, as observed with a crossed polarisers microscope in a thin cholesteric film sandwiched between (a, b) SiO_x evaporated surfaces, inducing a 30 degree pretilt, and (c, d) rubbed polyimide (SE1211), inducing a 60 degree pretilt. In both cases the texture is preserved for many days, even when the field is removed, but the ULH is lost if the temperature cycles through the isotropic phase or after the application of a large electric field which unwinds the helix.

symmetry of the homeotropic alignment, the direction for the helical axis is not defined and the ULH breaks down in domains that have a size comparable to the cell thickness. In order to exploit the ability of homeotropic alignment to favour the ULH texture, the surface also needs to break the rotational symmetry, as for instance in the method described in ref. 18, where the symmetry is broken by the periodic polymer walls.

An alternative approach is the use of periodic surface relief structures that match the periodicity of the bulk ULH. For instance, if one considers a cholesteric LC in contact with a $p/2$ periodic cusp-like surface structure inducing homeotropic alignment (see Fig. 5), finite difference numerical simulation based on Frank elasticity show that the ULH is the lowest energy texture.

5. Two Photon Absorption Laser-Lithography

A convenient way to experimentally test this idea is to use two photon excitation (TPE) laser-lithography [19] to create a micro-structured surface. The non linear nature of TPE allows producing structures with a submicron resolution.

This technique has already been used for LC alignment. Lee *et al.* [21] showed that surface gratings created using TPE photo-polymerization facilitate planar LC alignment. Here the TPE is used to create periodic surface reliefs structure to break

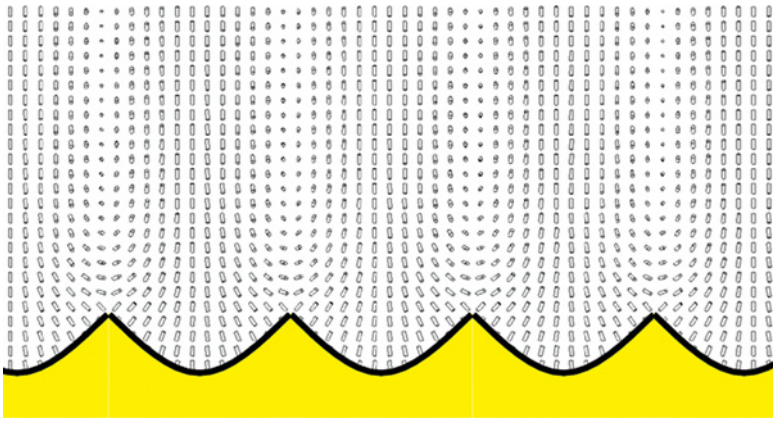

Figure 5. Director field of a short pitch cholesteric in contact with a p/2 periodic cusp-like surface structure, as obtained by finite difference numerical simulation based on Frank elasticity. (Figure appears in color online.)

the rotational symmetry of homeotropic alignment. The experimental setup for the fabrication process is schematically illustrated in Figure 6(a); the light source is a 790 nm laser with a repetition rate of 80 MHz (Newport Mai Tai); the beam is expanded and sent to a Spatial Light Modulator (SLM), which allows aberration correction; the beam is then sent to a large numerical aperture oil-immersion objective and focused on the sample; the sample is mounted on a xyz piezoelectric translation stage (see Fig. 6b). Similarly to ref. 21, the SRS were created using a curable photopolymer (Norland NOA 61) doped with a small amount (0.1% w/w) of bis(2,4,6-trimethylbenzoy) phenylphosphine oxide (Ciba Irgacure 819) to enhance the absorption at 400 nm. Also, a small amount (0.1% w/w) of fluorescent dye N,N'8-Bis(2,5-di-tert-butylphenyl)-3,4,9,10-perylene dicarboximide (BTBP) from Sigma-Aldrich was added to allow the visualization of the focal spot within the sample.

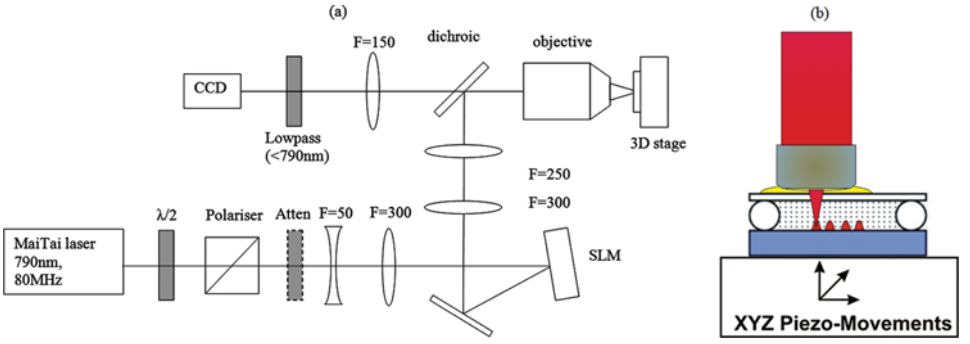

Figure 6. (a) Schematic diagram of the experimental setup for the fabrication process. (b) The sample is mounted on a xyz-piezoelectric translation stage and can be scanned under the high aperture objective used to focus the beam. (Figure appears in color online.)

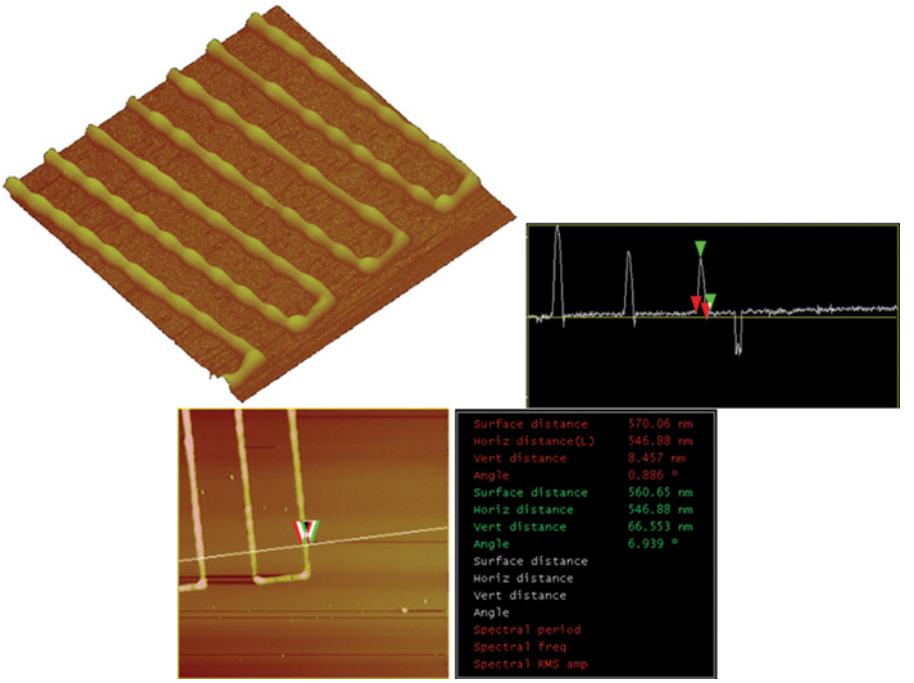

Figure 7. AFM measurements performed on the periodic surface structures. The lines are 2 μm spaced and their height is 0.1 μm. (Figure appears in color online.)

The material is sandwiched between two glass plates held together by the capillary action of the contained liquid. To allow the use of a high numerical aperture oil-immersion objective the upper substrate was 170 μm thick. The beam was focused and the structure created on the lower substrate, which was a standard ITO covered 1.1 mm thick glass plate. After TPE polymerization, the uncured material was removed by rinsing in acetone for 10 seconds, followed by rinsing in isopropanol for 30 seconds. AFM measurements were performed on micro-structured surfaces (see Fig. 7), showing for the cured structures a full-width well below a micron.

6. Periodic Surface Relief Structure Using TPE

Based on this method we prepared a test device with identical periodic surface structures that consisted of parallel lines, written on opposing substrates. The line spacing was 2 μm and the structure covered a $160 \times 160\,\mu m^2$ area. Before assembling the substrates, each surface was covered, by dip-coating, with a DMOAP (N;N-dimethyl-N-octadecyl-3-aminopropyltrimethoxysilyl chloride) monolayer, to promote homeotropic alignment. The test device was 8 μm thick and was filled with a cholesteric mixture (E7 + 0.25% R5011, Merck), having a 4 μm pitch, as determined by the Cano wedge method. A ULH texture formed (see Fig. 8a) as the sample was cooled down from the isotropic phase while applying a small ac field (10 kHz square wave). The electro-optical measurements performed on the test sample clearly

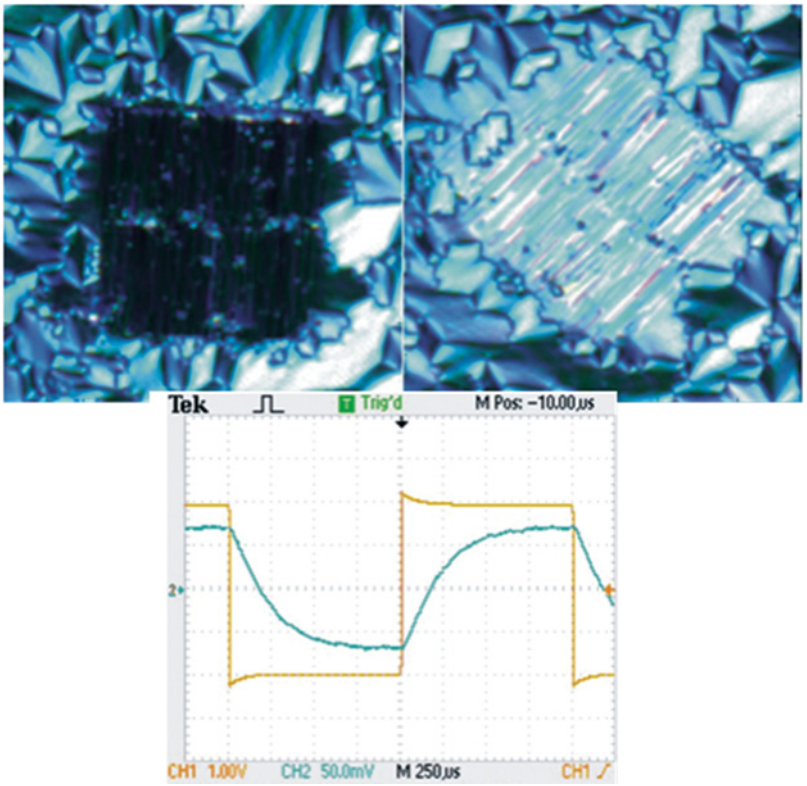

Figure 8. (a) test device as observed with a crossed polarisers microscope. As the sample was cooled down from the isotropic phase while applying a small ac field a ULH texture spontaneously formed. (b) Electro-optical measurement performed on the test device: intensity (blue line) transmitted through crossed polarisers. The lines of the surface relief structure make a angle of 22.5 degree with polarisers. As the polarity of the electric pulse (red line) is inverted, the transmitted intensity shows the asymmetric response typical of the FEO effect. (Figure appears in color online.)

show that the system was in the ULH texture (see Fig. 8b). The interesting aspect is that once the ULH was formed, it was stable even if the electric field is removed.

7. Modelling Cholesteric in Contact with a Micro-Structured Surface

In order to confirm that the ULH is stabilized by the micro-structured surface, we turned to theory and performed a Q-tensor based numerical simulation to search for the equilibrium structures corresponding to our system. The Q-tensor Q is a traceless, symmetric tensor used to characterise the orientational order within a liquid crystal. If we attach a unit vector $\hat{u}$ to each molecule the Q-tensor is given by $Q = < 3\ \hat{u}\ \hat{u} - \delta > /2$ where δ is the identity tensor and $< >$ represents an average over the molecular orientations. For a uniaxial system with director $\hat{n}$ and order parameter S the Q tensor is given by $Q = \mathrm{S} < 3\ \hat{n}\ \hat{n} - \delta > /2$. The Q-tensor formulation is particularly useful when modelling liquid crystal structures that contain defects. Adopting the familiar one elastic constant approximation the free energy

density of the liquid crystal can be written in terms of Q and the gradient operator as follows [22]

$$f = \left[\left(\frac{L_1}{9}\right)(\nabla_k Q_{ij})^2 + \left(\frac{4L_3}{9}\right)\varepsilon_{\alpha\beta\gamma}Q_{\alpha i}(\nabla_\beta Q_{\gamma i}) + \frac{(a+L_4)}{3}Q_{ij}Q_{ij} - \frac{4b}{9}Q_{ij}Q_{jk}Q_{ki} + \frac{c}{9}(Q_{ij}Q_{ij})^2\right].$$

By taking a uniaxial Q with order parameter S_{eq} we can identify the parameters L_1, L_3 and L_4 in terms of the Frank elastic coefficient K and the intrinsic chirality q_0 as follows

$$L_1 S_{eq}^2 = K; L_3 S_{eq}^2 = Kq_0; L_4 S_{eq}^2 = Kq_0^2,$$

while the order parameter S_{eq} is related to the thermotropic coefficients by

$$S_{eq} = \frac{b + \sqrt{b^2 - 4ac}}{2a}.$$

From a given starting condition we can evolve towards a local minimum of the free energy by simple relaxational dynamics [23]. We can then compare the final states produced for different starting conditions to assess their relative stability. We take K = 10pN, the pitch P = 1 μm, $q_0 = 2\pi \cdot 10^6\, m^{-1}$. Characteristic values for the thermotropic constants are $a = -1.2 \cdot 10^5\ Jm^{-3}$, $b = 5.6 \cdot 10^6\ Jm^{-3}$, $c = 9.3 \cdot 10^6\ Jm^{-3}$ which correspond to a uniaxial order parameter $S_{eq} = 0.62$. As is common in the Q-tensor approach taking such large values for the thermotropic coefficients results in defects that are very small compared with the typical length-scale for director variation. In order to resolve both length-scales it is then necessary to use a very fine computational grid, this rapidly becomes computationally expensive. In order to alleviate this problem we divide the thermotropic coefficients by a factor of 100, which increases the defect size by a factor of 10.

We first model a simple two dimensional rectangular system bounded by x = 0, x = P and y = −P, y = P. The substrates are at y = +/−P. We assume periodic boundary conditions in the x-direction while at the substrates we assume the Q-tensor is uniaxial with order parameter S_{eq} and with director aligned along the normal to the substrate (homeotropic anchoring). We consider two initial starting configurations for the bulk order parameter: 1) the Q-tensor describes a helix with a twist axis along the y-axis and with pitch P – this should lead to a Grandjean-type structure; 2) The Q-tensor describes a helix with a twist axis along the x-axis and with pitch P – this should lead to a ULH-type structure. Evolving these two initial states towards equilibrium and then calculating the final energy reveals that the pseudo-Grandjean type structure shown in Figure 9 is lower in energy.

In order to model the effects of surface relief we deform the two parallel substrates such that the point $(x, \pm P)$ on the initial substrate maps to $(x, \pm P[1 - \Delta\sin^8(q_0 x + \phi)])$. An illustration of this mapping is shown in Figure 10 for the case where $\phi = 0$. For boundary conditions we once again require that the order parameter is uniaxial at the substrates with order parameter S_{eq} and the uniaxial director is along the normal to the substrates. Applying a 5% surface perturbation, that is

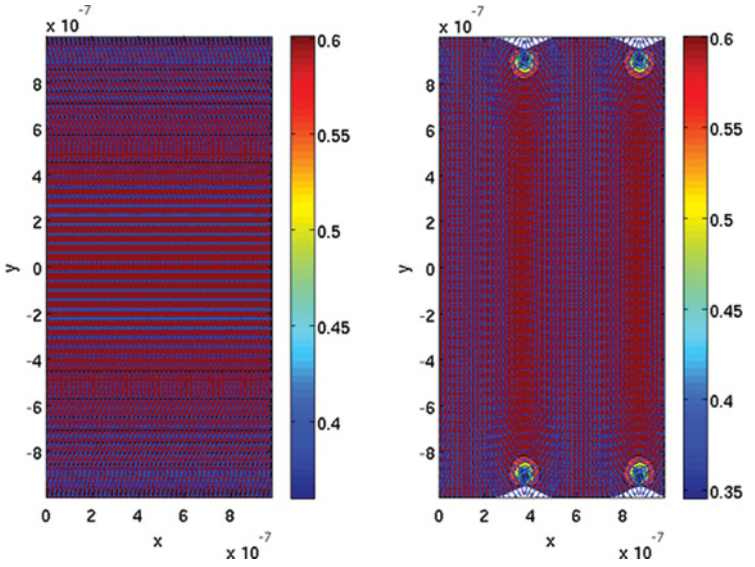

Figure 9. (a) The psuedo-Grandjean texture is the lower energy state for flat substrates. The blue arrows show the x and y components of the director while the background colour indicates the principal order parameter S according to colour bar shown. (b) With surface relief the ULH structure is the more stable. We clearly see the presence of strength $-\frac{1}{2}$ defects. (Figure appears in color online.)

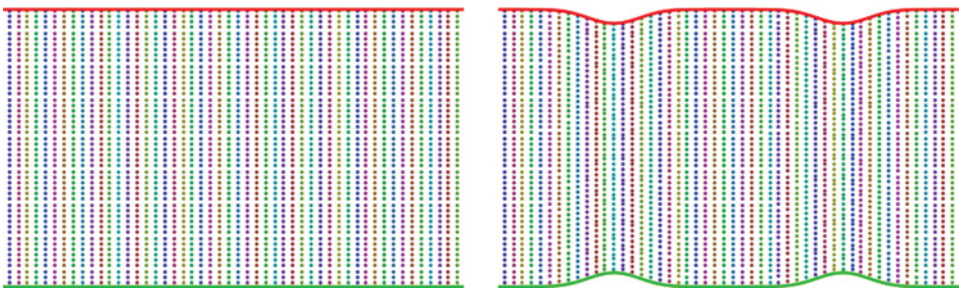

Figure 10. The rectangular grid on the left is transformed according to the map x, $y \rightarrow x$, $y\,[1 - 0.05\ \sin^8 q_0 x]$ generating the surface relief shown on the right. (Figure appears in color online.)

$\Delta = 0.05$ and evolving the same initial states we now find however that the ULH structure has a lower energy than the pseudo-Grandjean.

8. Conclusions

The use of micro-structured surface to align cholesteric LC in the ULH texture is a promising approach. Q-tensor based simulations predict that micro-structured aligning surfaces, having periodic relief matching the period of the cholesteric helix, promote the creation of a stable ULH texture. Polarized microscope observations, as

well as electro-optical measurements performed on a test device, prepared using TPE laser-lithography, shows that the periodic surface structure promotes a ULH texture which is stable also when the electric field, used to form it, is removed. On the other hand, the quality of the texture is not yet satisfying and the method is not viable to create a large area device. We believe that the quality of the texture can be improved with a more precise registration of the two aligning substrates. To allow the fabrication of larger area of surface structure we are considering the use of other techniques such as UV-lithography, IB milling and Nanoimprinting Lithography.

Further work need to be done to determine the effect of the mismatch between the surface and the bulk periodicity.

Finally, some caution is required on extrapolating these results back to a situation involving the short pitch materials appropriate for electro-optic applications. While the device thickness, and minimum dielectric coherence length λ_d prior to helix unwinding, are scaled in a manner analogous to the pitch, both the anchoring extrapolation length L and the nematic coherence length λ_n remain constant [22]. The assumption of rigid anchoring is justified in our work since both the pitch p and the minimum dielectric coherence length λ_d are a few orders of magnitude larger than the anchoring extrapolation length L, which for standard surface alignment materials is smaller than 100 nm.

Acknowledgment

The authors want to thank the UK EPSRC for financial support, and Merck for providing the liquid crystalline materials. This work was also partially supported by the UK Engineering and Physical Sciences Research Council (EP/F013787/1).

References

[1] Meyer, R. B. (1969). *Phys. Rev. Lett.*, *22*, 918.
[2] Patel, J. S., & Meyer, R. B. (1987). *Phys. Rev. Lett.*, *58*, 1538.
[3] Rudquist, P., Komitov, L., & Lagerwall, S. T. (1994). *Phys. Rev. E*, *50*, 4735.
[4] Rudquist, P., Carlsson, T., Komitov, L., & Lagerwall, S. T. (1997). *Liq. Cryst.*, *22*, 445.
[5] Rudquist, P., Komitov, L., & Lagerwall, S. (1998). *Ferroelectrics*, *213*, 447.
[6] Musgrave, B., Coles, M., Perkins, S., & Coles, H. (2001). *Mol. Cryst. Liq. Cryst.*, *366*, 2587.
[7] Blatch, A., Coles, M., Musgrave, B., & Coles, H. (2003). *Mol. Cryst. Liq. Cryst.*, *401*, 161.
[8] Coles, H., Clarke, M., Morris, S., Broughton, B., & Blatch, A. (2006). *J. Appl. Phys.*, *99*, 034104.
[9] Morris, S. M., Cho, Y., Pivnenko, M. N., & Coles, H. J. (2007). *J. Appl. Phys.*, *101*, 114109.
[10] Lagerwall, S. T., & Stebler, B. (1995). *SPIE*, *2372*, 59.
[11] Rudquist, P., Buivydas, M., Komitov, L., & Lagerwall, S. T. (1994). *J. Appl. Phys.*, *76*, 7778.
[12] Patrick Salter, S., Giovanni, Carbone, Sharon Jewell, A., & Steve Elston, J., Peter, Raynes. (2009). *Phys. Rev. E*, *80*, 041707.
[13] Rudquist, P., Komitov, L., & Lagerwall, S. T. (1998). *Liq. Cryst.*, *24*, 329.
[14] Kim, S., Chien, L., & Komitov, L. (2005). *Appl. Phys. Lett.*, *86*, 161118.
[15] Broughton, B., Clarke, M., Morris, S., Blatch, A., & Coles, H. (2006). *J. Appl. Phys.*, *99*, 023511.

[16] Robert Meyer, B., & Jayantilal Patel, S. *"Flexoelectric liquid crystal device" US patent* 4917475, Mar 6, 1987.
[17] Komitov, L., Bryan-Brown, G., Wood, E., & Smout, A. (2010). *J. Appl. Phys. 86, 3508, (1999); Hegde, G., & Komitov, L., Appl. Phys. Lett.*, *96*, 113503.
[18] Carbone, G., Salter, P., Elston, S., Raynes, P., De Sio, L., Ferjani, S., Strangi, G., Umeton, C., & Bartolino, R. (2009). *Appl. Phys. Lett.*, *95*, 011102.
[19] Kawata, S., Sun, H., Tanaka, T., & Takada, K. (2001). *Nature*, *412*, 697.
[20] Corbett, D., Carbone, G., & Elston, S. J. *unpublished.*
[21] Lee, C. H., Yoshida, H., Miura, Y., Fujii, A., & Ozaki, M. (2008). *Appl. Phys. Lett.*, *93*, 173509.
[22] de Gennes, P. G. (1975). *The Physics of Liquid Crystals*, Clarendon Press: Oxford.
[23] Sonnet, A. M., & Virga, E. G. (2001). *Phys. Rev. E*, *64*, 031705.